DR. DONG FU (Orcid ID : 0000-0002-6865-5033)

Article type : Original

Tumor-selective altered glycosylation and functional attenuation of CD73 in human hepatocellular carcinoma

Karel P. Alcedo[1], Andres Guerrero[2],Venkatesha Basrur[3], Dong Fu[1], Monea L. Richardson[1], Joshua S. McLane[1], Chih-Chiang Tsou[5], Alexey I. Nesvizhskii[3,5], Theodore H. Welling[4], Carlito B. Lebrilla[2], Carol A. Otey[1], Hong Jin Kim[6], M. Bishr Omary[7,8] and Natasha T. Snider[1§]

[1]Department of Cell Biology and Physiology, University of North Carolina at Chapel Hill

[2]Department of Chemistry, University of California Davis

[3]Department of Pathology, University of Michigan

[4]Perlmutter Cancer Center and Department of Surgery, NYU Langone Health, New York, NY

[5]Department of Computational Medicine and Bioinformatics, University of Michigan

[6]Department of Surgery, University of North Carolina at Chapel Hill

[7]Department of Molecular & Integrative Physiology, University of Michigan

[8]Department of Medicine, University of Michigan

[§]Corresponding Author:

Natasha Snider, University of North Carolina - Chapel Hill, Department of Cell Biology and Physiology, 5340C MBRB, 111 Mason Farm Rd, Chapel Hill NC 27516, Tel: (919) 962-6033, e-mail: ntsnider@med.unc.edu

The authors declare there are no conflicts of interest.

Author contributions: study concept and design (NTS, MBO); acquisition of data (KPA, AG, VB, DF, MLR, NTS); analysis and interpretation of data (KPA, AG, VB, DF, MLR, JSM, CCT; MBO, NTS); drafting of the manuscript (KPA, NTS); critical revision of the manuscript for important intellectual content (THW, CL, AG, VB, AN, CAO, HJK, MBO); obtained funding (NTS, MBO, KPA, AN); study supervision (MBO, NTS).

Funding sources: This work was supported by NIH grants DK110355 (to NTS), DK47918 (to MBO), GM094231 (to A.N.), and institutional NIH grants to UNC (DK034987) and to the University of Michigan (DK034933 and CA210967). The study was also supported by institutional training grants from the UNC Cancer Cell Biology Training Grant Program (to KPA) and UNC PREP (to MLR).

List of Abbreviations: AMP, adenosine monophosphate; **AR,** adenosine receptor; **ATP,** adenosine triphosphate; **CD73,** ecto-5′-nucleotidase; **CF102,** -chloro-N6-(3-iodobenzyl)-adenosine-5'-N-methyl-uronamide; **EndoH,** endoglycosidase H; **ER,** endoplasmic reticulum; **FPKM,** fragments per kilobase of exon model per million reads mapped; **GPI-AP,** glycosylphosphatidylinositol-anchored protein; **HCC,** hepatocellular carcinoma; **PNGaseF,** Peptide -*N*-Glycosidase F; **TCGA,** The Cancer Genome Atlas; **TNAP,** tissue non-specific alkaline phosphatase.

ABSTRACT

CD73, a cell-surface *N*-linked glycoprotein that produces extracellular adenosine, is a novel target for cancer immunotherapy. Although anti-CD73 antibodies have entered clinical development, CD73 has both pro- and anti-tumor functions, depending on the target cell and tumor type. The aim of this study was to characterize CD73 regulation in human hepatocellular carcinoma (HCC). We examined CD73 expression, localization, and activity using molecular,

biochemical, and cellular analyses on primary HCC surgical specimens, coupled with mechanistic studies in HCC cells. We analyzed CD73 glycan signatures and global alterations in transcripts encoding other *N*-linked glycoproteins using mass spectrometry glycomics and RNAseq, respectively. CD73 was expressed on tumor hepatocytes, where it exhibited abnormal *N*-linked glycosylation, independent of HCC etiology, tumor stage, or fibrosis presence. Aberrant glycosylation of tumor-associated CD73 resulted in a 3-fold decrease in 5′-nucleotidase activity ($p<0.0001$). Biochemically, tumor-associated CD73 was deficient in hybrid and complex glycans specifically on residues N311 and N333, located in the C-terminal catalytic domain. Blocking N311/N333 glycosylation via site-directed mutagenesis produced CD73 with significantly decreased 5′-nucleotidase activity *in vitro*, similar to the primary tumors. Glycosylation-deficient CD73 partially co-localized with the Golgi structural protein GM130, which was strongly induced in HCC tumors. RNAseq analysis further revealed that *N*-linked glycoprotein-encoding genes represented the largest category of differentially expressed genes between HCC tumor and adjacent tissue. Conclusion: We provide the first detailed characterization of CD73 glycosylation in normal and tumor tissue, revealing a novel mechanism that leads to the functional suppression of CD73 in human HCC tumor cells. The present findings have translational implications for therapeutic candidate antibodies targeting cell-surface CD73 in solid tumors and small-molecule adenosine receptor agonists that are in clinical development for HCC.

Ecto-5′-nucleotidase (CD73) is the major enzyme that dephosphorylates extracellular adenosine 5'-monophosphate (AMP) to produce adenosine. CD73 activity is ubiquitous in mammalian systems, and regulates purine salvage and purinergic signaling in tissue homeostasis, inflammation, fibrosis, and cancer (1, 2). CD73-generated adenosine can suppress anti-tumor T-cell responses, thereby promoting the progression of breast, skin, ovarian, and prostate cancer in animal models (3). Several anti-CD73 inhibitory antibodies (MEDI9447, CPI-006, TJ004309) are currently undergoing clinical testing for advanced solid tumors (4, 5). However, the role of CD73 in cancer is complex because CD73 activity is crucial for protecting endothelial and epithelial barrier functions (6), particularly during hypoxic conditions (7, 8) and CD73 protects the epithelial integrity in well-differentiated early stage endometrial carcinoma, which is associated with better overall patient survival (9). This clearly demonstrates that the role of CD73 in cancer is not uniform and warrants a critical mechanistic evaluation of CD73 regulation and function at multiple levels and in different cancer types (6).

CD73 is a known regulator of hepatocyte injury (10, 11) and fibrogenic responses in the liver (12, 13), but its functional regulation in liver cancer has not been investigated to date. Given the importance of CD73 as a novel target for cancer therapy, and the significant disease burden of liver cancer (14), the aim of the present study was to investigate the regulation and activity of CD73 protein in human HCC. CD73 is widely expressed in hepatobiliary malignancies, and aberrant intense cytoplasmic CD73 staining is a marker of invasive lesions in hepatocellular carcinoma (HCC) (15). The mechanism behind the aberrant CD73 localization, and whether it is enzymatically active, is not known. Novel interventions for HCC are critically needed, and modulation of adenosine signaling represents one potential strategy. Specifically, the adenosine-A3 receptor (A_3R) is highly expressed in HCC, and its activation by a selective agonist (CF102), has antitumor effects in a rat model of HCC (16). CF102 (namodenoson) recently completed phase II clinical testing and showed a favorable clinical safety profile and a positive signal of efficacy in patients with advanced HCC and severe liver dysfunction, justifying further testing in phase III trials (17, 18). In light of the important role of adenosine signaling as a clinical target in

HCC, it is critical to understand how the activity of the major extracellular AMPase, CD73, is regulated in HCC tumors.

As a glycosylphosphatidylinositol-anchored protein (GPI-AP), CD73 undergoes complex processing via the secretory pathway (19). Proteins destined for this pathway undergo initial maturation in the endoplasmic reticulum (ER), followed by vesicular transport through the Golgi apparatus before being targeted to their ultimate destinations via the *trans*-Golgi network. A key regulatory step in the proper execution of this process is the sequential covalent modification of proteins with oligosaccharides linked via asparagine residues, termed *N*-linked glycosylation (20). Alterations in the *N*-linked glycoproteome are hallmarks of many cancers, including HCC (21). In this study, we reveal a novel glycosylation mechanism leading to the mislocalization and functional suppression of CD73 in HCC tumors. Our results illuminate specific regulatory mechanisms that may be exploited for targeted treatment to improve HCC patient outcomes.

EXPERIMENTAL PROCEDURES

Antibodies and Reagents: Mouse anti-Flag M2 clone (Sigma-Aldrich) and rabbit anti-CD73 clone HPA017357 (Atlas Antibodies) were used to detect tagged and untagged (endogenous) CD73, respectively. Mouse anti-CD73 clone AD2 (BD Biosciences) was used for immunoprecipitation of CD73. Mouse anti-CD73 clone IE9 (Santa Cruz Biotechnology) was used to co-stain with tight junction markers ZO1 (rabbit; Cell Signaling) and Claudin-1 (rabbit; ThermoFisher Scientific). Other antibodies used were: rat anti-K19 (Troma-III; Developmental Studies Hybridoma Bank), rabbit anti-TNAP (Abcam) and mouse monoclonal antibodies for Golgi marker proteins GM130, Vti1, STx6, and GS27 (BD Biosciences). cDNA encoding human *NT5E*-1 and *NT5E*-2 in pCMV6-Entry and control empty vector were purchased from Origene. EndoH and PNGase F glycosidases were used with liver lysates as recommended by the manufacturer (New England Biolabs).

Human specimens: Surgical specimens were collected under approved human subjects protocols at the University of Michigan (UM) and the University of North Carolina at Chapel Hill (UNC). HCC surgical specimens that were collected at UM were described previously (22).

Normal human liver specimens were from surgical resections of unaffected liver tissue, collected during removal of colorectal cancer metastasis to the liver. An additional 27 liver-tumor pairs of HCC surgical specimens (23 of which were CD73-positive) were collected at UNC under an approved human subjects protocol (clinical information provided Supporting File 1).

Cell culture, transfections, imaging, immunoblotting, and qPCR. The Huh7 cells were obtained from the Japanese Collection of Research Bioresources (JCRB) and cultured in DMEM supplemented with 10% fetal bovine serum and 100U/mL penicillin/streptomycin. PLC/PRF5 cells were from the American Type Culture Collection (ATCC; Manassas, VA) and cultured according to the ATCC recommendations. Site-directed mutagenesis was performed using the QuikChange kit (Agilent Technologies). For immunofluorescence analysis, the human tissues or cells were fixed in methanol at -20°C for 10 minutes, washed three times in PBS and incubated in blocking solution (2.5% bovine serum albumin, 2% normal goat serum in PBS) for 1 hour at room temperature. Primary antibodies were diluted in blocking buffer and incubated overnight at 4°C. Following three PBS washes, the cells/tissues were incubated with Alexa Fluor-conjugated secondary antibodies diluted in blocking solution for 1h at room temperature, followed by DAPI incubation for 5 minutes, and mounted in Fluoromount-G (SouthernBiotech, Birmingham, AL) overnight. Secondary antibodies alone served as negative controls. Zeiss 880 confocal laser scanning microscope using a 63x (1.4 NA) oil immersion objective (Zeiss, Jena, Germany) was used for imaging.

Biochemical assay of CD73 expression and activity. CD73 was extracted from cell or liver tissue homogenates in 50mM *n*-octylglucoside (Sigma) in PBS (OG lysis buffer) with freshly added complete protease inhibitor cocktail (Roche) and shaking for 2 hours at 4°C, followed by centrifugation at 20,000g for 20min. Immunoprecipitation of CD73 from OG lysates was performed using Dynabeads protein G (ThermoFisher Scientific) following manufacturer instructions. Measurement of 5′-nucleotidase activity was performed using a commercial kit (Diazyme) with OG liver lysates that were first normalized to 1mg/mL total protein concentration. This assay is based on a four-reaction sequence, beginning with the enzymatic hydrolysis of 5'-inosine monophosphate (5'-IMP) to form inosine, which is subsequently converted to hypoxanthine by purine nucleoside phosphorylase (PNP). Xanthine oxidase (XOD) converts hypoxanthine to uric acid and hydrogen peroxide (H_2O_2). H_2O_2 is then reacted with N-

Ethyl- N-(2-hydroxy-3-sulfopropyl)-3-methylaniline and 4- aminoantipyrine in the presence of peroxidase to generate a quinone dye, which is monitored in a kinetic manner. The specificity of the 5'-IMP-based assay for CD73 activity was originally described in multiple tissues (8), and specifically in the liver using $CD73^{-/-}$ liver lysates (11).

Mass spectrometry analysis of site-specific CD73 glycosylation and determination of glycan structures. CD73 was immuno-depleted from liver and tumor OG lysates and subjected to mass spectrometry analysis to determine site-specific glycosylation and glycan structures. The band corresponding to CD73 protein was excised and destained with 30% methanol for 4 h. Upon reduction (10 mM DTT) and alklylation (65 mM 2-Chloroacetamide) of the cysteines, proteins were digested overnight with sequencing grade, modified trypsin (Promega). Resulting peptides were resolved on a nano-capillary reverse phase column (Acclaim PepMap C18, 2 micron, 15 cm, ThermoScientific) using a 1% acetic acid/acetonitrile gradient at 300 nl/min and directly introduced in to Orbitrap Fusion tribrid mass spectrometer (Thermo Scientific, San Jose CA). MS1 scans were acquired at 60K resolution. Data-dependent high-energy C-trap dissociation MS/MS spectra were acquired with top-speed option (3 sec) following each MS1 scan (relative CE ~35%). Fragment (daughter) ion masses were measured in orbitrap (resolution of 15K). XX Peptide identification and Site-specific glycan structures were determined using the program GP Finder, as described previously (23). To determine glycopeptide abundance, we used the summation of elution apex intensities of all MS1 isotope peaks.MS1 precursor features of glycopeptides were extracted by feature detection algorithm described in DIA-Umpire (24). Feature detection was restricted to +3, +4 and +5 charge states and have 3-5 isotope peaks. For each LC-MS run, the detected features with close precursor m/z (± 20 ppm) and charge state identical to the identified glycopeptides were considered as the candidate features for quantification. For the identified glycopeptides, the feature closest to identified retention time was extracted. If a glycopeptide was only identified in other LC-MS runs, the most intense candidate feature within 2 min retention time range of the identified retention times from other LC-MS runs was extracted.

RNAseq analysis of differentially expressed genes in non-tumor adjacent and HCC tumor tissue. Surgical tissues from 2 adjacent liver-tumor pairs (where tumor CD73 displayed shift in migration on SDS-PAGE gel) were preserved in RNAlater. RNA was extracted using the

RNeasy kit (Qiagen) and used for sequencing analysis (all RIN values were >9). For the published study, SRA data files were obtained from NCBI GEO repository (GSE 33294), and converted into fastq files. Quality of the raw reads data was determined using FastQC. The software package Tuxedo Suite was used for alignment, differential expression analysis, and post-analysis diagnostics. FastQC for a second round of quality control (post-alignment), to ensure that only high quality data would be input to expression quantitation and differential expression analysis. We used Cufflinks/CuffDiff (version 2.1.1) for expression quantitation and differential expression analysis, using UCSC hg19.fa as the reference genome sequence and UCSC hg19.gtf as the reference transcriptome annotation. We identified genes and transcripts as being differentially expressed based on three criteria: test status = "OK", FDR < 0.05 and fold change ≥ 1.5. We annotated genes and isoforms with NCBI Entrez GeneIDs and text descriptions. We further annotated differentially expressed genes with Gene Ontology (GO) [6] terms using NCBI annotation. We used DAVID (version 6.7) for enrichment analysis of the set of differentially expressed genes to identify significantly enriched functional categories, which are presented in Supporting File 2.

RESULTS

CD73 is expressed in malignant hepatocytes and exhibits cytoplasmic distribution in HCC tumors. Using data from the PanCancer Atlas Consortium (25) we determined that the CD73-encoding gene (*NT5E*) did not correlate with a specific tumor immune sub-type in HCC (Fig.1A). However, aside from its functions in the immune system, CD73 is also well-known regulator of epithelial cells (6), including hepatocytes (11). Therefore, we investigated CD73 protein expression and localization in non-diseased (normal) liver and HCC tumor and adjacent non-tumor tissues. Immunofluorescence imaging revealed abundant CD73 expression in normal liver and in HCC (Fig.1B). CD73 in HCC adjacent and tumor tissue appeared largely intracellular (Fig.1B). Co-staining with the tight junction marker ZO1 revealed CD73 presence in the cytoplasm as well as the lumen of bile canaliculi in adjacent liver and primarily cytoplasmic and perinuclear distribution in the tumor tissue (Fig. 1C). To determine which epithelial cell types express CD73 in HCC tumors, we co-stained for the epithelial markers keratin 8 and keratin 19. As shown in Fig.1D, CD73 is abundant in K8-positive, but not K19-positive cells,

suggesting that it is expressed primarily on malignant hepatocytes and absent from tumor cholangiocytes. By immunoblot analysis, we detected CD73 protein in all HCC cell lines we tested (Hep3B, Huh7, MHCC97, SNU-423, and SNU-449), while PLC/PRF/5 hepatoma cells were CD73-negative (Fig.2A). Immunofluorescence analysis confirmed lack of CD73 in the PLC/PRF5 cells (Fig.2B) and revealed cytoplasmic and membranous distribution of CD73 in the Huh7 cells (Fig.2B-C). Specifically, co-staining with the tight junction markers ZO1 and claudin-1 showed CD73 localization within the lumen of small bile canaliculi-like structures (Fig. 2C, arrows) that Huh7 cells are known to form in culture (26), as well as presence of CD73 in perinuclear puncta (Fig.2C, arrowheads), similar to its distribution in the primary HCC tissues.

Tumor-specific biochemical changes on CD73 correlate with decreased 5′-nucleotidase activity. HCC typically develops in the context of cirrhosis, so we asked whether CD73 protein expression is different in the tumor versus the non-tumor adjacent tissue. Immunoblot analysis (Fig.3A) and quantification of band intensities from 23 CD73-positive HCC liver-tumor pairs (Fig.3B; Supporting File 1) revealed heterogeneous expression of CD73. Of the 23 tumors, CD73 was increased in 11, unchanged in 6, and decreased in 6 tumors, relative to adjacent liver. However, we also noted that in 13/23 (57%) of the CD73-positive liver-tumor pairs, CD73 from the tumor tissue migrated faster on SDS-PAGE gels compared to CD73 from non-tumor adjacent liver, as shown by the representative immunoblot in Fig. 3C. Tumor-associated biochemical changes in CD73 were independent of HCC etiology, tumor stage, and presence of fibrosis (Fig.3D-F). However, altered biochemical processing of CD73 in the HCC tumors was associated with significantly decreased enzymatic activity (Fig.3G). Although there was a negative correlation trend between CD73 shift and disease-free status (p=0.20) or patient survival (p=0.28) it was not statistically significant (Supplemental Fig.1A-C). Similarly, total tumor CD73 expression did not correlate with clinical outcomes based on the samples tested here (Sup Fig. 1 D-F).

CD73 undergoes differential glycosylation in HCC tumors relative to non-tumor adjacent tissue. CD73 has four consensus *N*-glycosylation motifs: ^{53}NAS, ^{311}NSS, ^{333}NYS, and ^{403}NGT (Fig.4A), and changes in glycosylation at one or more of these sites may alter CD73 activity since three of them (N311/N333/N403) are located in the C-terminal catalytic domain of the molecule (19). Therefore, we tested the hypothesis that tumor CD73 undergoes altered

glycosylation. To that end, we de-glycosylated CD73 *in vitro* using EndoH (typically removes immature high mannose glycans introduced in the ER) and PNGase F (removes more mature complex glycans introduced post-ER exit). The differential migration on the gel was not present after PNGase F treatment, but still present in the EndoH-resistant fraction (Fig. 4B). This suggested that glycosylation differences on tumor CD73 are introduced after exit from the ER. Mass spectrometry glycomics analysis revealed that the majority of CD73 glycans are conjugated to N311 and N333, followed by N403 and N53 (Fig. 4C). While N333 was conjugated primarily to complex glycans, N311 displayed a mix of high mannose, hybrid, and complex glycans (Fig. 4D). Globally, the major glycosylation differences on CD73 from HCC tumors were in specific glycan structures, with significant increase in high mannose glycans and decrease in hybrid glycans (Fig. 5A). The greatest glycosylation changes were observed at site N311 (Fig.5B), where under normal conditions high mannose glycans accounted for <20% of all glycans, while in tumor CD73 this residue was highly mannosylated (>60% of total glycans). In addition, incorporation of complex glycans was significantly reduced at both the N311 and N333 sites (Fig. 5B-C).

Site-specific glycosylation regulates CD73 enzymatic activity and sub-cellular distribution. To assess the functional significance of site-specific CD73 *N*-glycosylation, we generated non-glycosylatable mutants (N311Q and N333Q) and compared their enzymatic activity to WT CD73 (Fig. 5D). The glycosylation-deficient N311Q and N333Q mutants had 30% and 50% lower enzyme activity, respectively, compared to WT CD73. Furthermore, the subcellular distribution of both mutants appeared predominantly perinuclear compared to WT CD73 (Fig. 5E). To assess whether the intracellular CD73 puncta co-localize with the Golgi organelle, where most of the hybrid and complex glycans are conjugated to proteins, we co-stained with the Golgi marker GM130. As shown in Fig.5F, the glycosylation- and catalytically-deficient N333Q mutant partially co-localized with GM130, suggesting that it is partly retained in the Golgi compartment. Combined, these data demonstrate that *N*-glycosylation of CD73 at N311 and N333, the two sites that are aberrantly glycosylated on CD73 in primary HCC tumors, is critical for CD73 function.

Upregulation of Golgi protein GM130 and global differences in the expression of genes encoding *N*-linked glycoproteins in HCC tumors. We analyzed major proteins that regulate the transit of GPI-APs through the Golgi organelle, including: GM130, which is important for

glycosylation and maintenance of Golgi structure, the v-SNARE (Vti1) and t-SNARE (syntaxin-6) proteins involved in vesicle transport through the Golgi, and a SNAP receptor that regulates protein transport in the Golgi (GS27). GM130 exhibited the most profound differences between tumor and non-tumor adjacent tissue, and was upregulated more than 8-fold in HCC tumors (Fig.6 A-B). While in non-tumor adjacent human liver tissue GM130 staining appeared as perinuclear puncta, in HCC tumors the puncta appeared enlarged and merged, forming larger structures (Fig. 6C).

RNAseq analysis was performed on two pairs of HCC specimens (adjacent and tumor tissue) that displayed differences in CD73 migration on gel, as shown in insets to Fig.6E. We additionally analyzed gene expression data on two HCC liver-tumor pairs from a published RNAseq dataset (GSE 33294). These results revealed that *N*-linked glycoprotein-encoding genes were among the most represented category of differentially expressed genes (Fig. 6D and Supporting File 2). Since ecto-nucleotidases that act upstream of CD73 in the liver (e.g. ENPP2, ENTPD8) (27) and A_3R, are also *N*-glycosylated, we compared their gene expression levels in non-tumor versus tumor tissue from the RNAseq sets. This comparison revealed a general decrease in expression (11-95%) in the tumors compared to adjacent liver (Fig.6E). Taking into account the RNAseq results and the molecular and biochemical studies, we propose a potential model for a tumor-selective mechanism to limit extracellular adenosine signaling in HCC tumors via: (i) disruption of CD73 glycosylation leading to diminished activity; and (ii) transcriptional downregulation of ecto-nucleotidases supplying the AMP substrate of CD73, such as ENTPD8 (Fig. 6F).

DISCUSSION

CD73 as a potential target in HCC. HCC accounts for the vast majority of primary liver cancer cases, and there are ~850,000 new cases diagnosed worldwide each year (28). Recent trends in the U.S. reveal that, while death rates continue to decline for most cancer types, liver cancer mortality has continued to increase at a rate of 2.5-3% per year and 5-year survival remains below 20% (29). At the onset of symptoms, HCC is typically advanced and not amenable to current treatment approaches, which are very limited. Direct modulation of adenosine receptor

activity represents a promising therapeutic strategy for HCC patients (17). In addition to direct-acting agonists, such the clinical candidate A_3R agonist CF102, an alternative approach is to augment the generation of the endogenous ligand, adenosine. Here we demonstrate that the adenosine-generating function of CD73 is compromised in human HCC tumors due to aberrant *N*-linked glycosylation. Aside from revealing a novel mechanism in HCC tumor biology, our results may potentially help to identify patients who are more likely to benefit from A_3R agonists, based on their tumor CD73 glycosylation status, localization and activity. While our primary focus here was on tumor hepatocytes and HCC cells, the regulation and function of CD73 on other cell types, such as endothelial cells and lymphocytes, will need to be taken into account in future studies to determine if CD73 augmentation or blockade could be of potential benefit to HCC patients.

Differences in CD73 regulation and function across cancer types. Tumor-selective transcriptional upregulation of *NT5E* can be pro-tumorigenic, as high expression of epithelial CD73 is associated with low levels of tumor-infiltrating leukocytes and reduced disease-free and overall survival in triple negative breast cancer (30). However, in contrast to breast cancer, CD73 is significantly downregulated in advanced endometrial tumors compared to normal endometrium and less aggressive tumors (6, 9), similar to invasive bladder cancer (31, 32) and in both cases high expression predicts more favorable patient outcome. In the case of endometrial cancer, downregulation of CD73 is detrimental, as it leads to compromised integrity of the epithelial barrier. Specifically, CD73-generated adenosine is necessary for the A_1R receptor-dependent cortical actin polymerization and cell-cell adhesion (9). Our results herein reveal that post-translational modulation of the CD73 nucleotidase function via *N*-linked glycosylation is yet another important, but underappreciated mechanism for modulating CD73 function. Given our findings, assessment of CD73 expression by tissue staining alone does not necessarily reflect presence of the active enzyme, as more detailed biochemical studies are needed to probe that function. Resolving which mode of CD73 regulation is most relevant for the specific tumor type will aid in understanding which cancer patients are likely to benefit from CD73 blocking antibodies.

The need for robust preclinical in vivo studies on the role of CD73 in HCC. Studies examining how CD73 loss impacts HCC development in rodent models have not been performed, with the

exception of a limited analysis reporting that subcutaneous inoculation of MHCC97-derived tumors showed decreased growth in $CD73^{-/-}$ compared to WT mice (33). Use of global and tissue-specific CD73 knockout models in combination with standard HCC induction models, such as chemical carcinogenesis, fatty liver disease, and alcohol-induced liver disease (34) will help address this question in a rigorous manner in future studies. One major caveat is that CD73 regulation in humans is different from rodents, as we have shown to be the case with the post-transcriptional processing of the *NT5E* gene, which is uniquely spliced in humans compared to all other species (22). Therefore, the use of humanized mice and patient-derived xenograft mouse models will likely be warranted.

Post-transcriptional and post-translational regulation mechanisms alter CD73 functions. Our prior and current results demonstrate that the major mechanism of CD73 regulation in HCC is not transcriptional, but post-transcriptional (22) and post-translational (current study). Previously we demonstrated that alternative splicing generates a novel human-specific CD73 isoform in cirrhosis and HCC (CD73S), which is present in both non-tumor adjacent and tumor tissue and acts in a dominant-negative fashion (22). Our current results provide additional evidence that the activity of the major, canonical CD73 protein is selectively altered by *N*-linked glycosylation to produce a highly mannosylated, enzymatically impaired glycoform in HCC tumors. Understanding the pathways that lead to these changes may reveal additional molecular targets to elevate CD73 activity selectively in HCC tumors. For example, restoration of Golgi morphology and glycosylation has been shown to enhance the susceptibility of prostate cancer cells to apoptosis (35) and similar approaches may be explored in HCC. Our results may also help explain several previously reported functions of CD73 in multiple cell types that are independent of its activity as an AMPase, such as: T-cell activation via protein-protein interactions to deliver a co-stimulatory signal (36), promoting adhesion of lymphocytes to the endothelium (37), conferring resistance to apoptosis of leukemia cells (38) and inducing phosphorylation of intracellular proteins in response to antibody ligation (39, 40). Therefore, it is plausible that *N*-linked glycosylation is a mechanism to tune adenosine-independent CD73 functions in different cell types under physiological and disease states.

CD73 as a marker of Golgi organelle dysfunction in HCC tumors. The significant and selective upregulation of GM130 in HCC tumors implicates the Golgi organelle in HCC tumor biology.

The Golgi apparatus is the central compartment of the secretory pathway, where proteins and lipids are extensively modified as they traverse the organelle *en route* to their intended destination to cellular membranes or to being secreted outside the cell. Proper architecture of the Golgi, which is composed of stacks of cisternae, ensures that the various enzymes involved in the modification of proteins and lipids are localized to their proper compartment. The Golgi structural protein GM130 is critical for the lateral linking of Golgi elements, which in turn ensures the proper localization of glycosylation enzymes (41). It was shown previously that downregulation of GM130 had anti-tumor effects in a mouse model of lung cancer (42). Presently it is not clear what causes the Golgi alterations in cancer, but it is known that many genes, in particular kinases, exert control of this important organelle (43). Therefore, the mechanism behind the upregulated GM130 expression in HCC tumors remains to be in investigated, and it may involve kinome-level changes.

N-linked glycosylation as a mechanism for HCC progression. Previous studies aimed at identifying serum biomarkers reported major HCC-associated alterations in the types and abundance of glycans on specific serum proteins, such as α-fetoprotein and GP73 (44-47). Aside from being a biomarker of HCC, altered *N*-glycosylation can also serve a functional role to promote HCC tumor metastasis. For example, altered *N*-glycan branching of CD147 enhances its binding to β1-integrin to promote HCC tumor metastasis (48). While the functional significance of elevated high-mannose glycans that we identified on HCC tumor CD73 is not clear presently, global high mannose glycosylation negatively affects multiple essential functions of the intestinal epithelium, such as permeability, host-microbe interactions and the activities of membrane-associated proteins (49). Therefore, it is plausible that the highly mannosylated CD73 tumor glycoform blocks the tissue barrier function of CD73 (6), which will be a key question for future studies.

References

1. Zimmermann H, Zebisch M, Strater N. Cellular function and molecular structure of ecto-nucleotidases. Purinergic Signal 2012;8:437-502.

2. Ipata PL, Balestri F. The functional logic of cytosolic 5'-nucleotidases. Curr Med Chem 2013;20:4205-4216.

3. Antonioli L, Yegutkin GG, Pacher P, Blandizzi C, Hasko G. Anti-CD73 in cancer immunotherapy: awakening new opportunities. Trends Cancer 2016;2:95-109.

4. Hay CM, Sult E, Huang Q, Mulgrew K, Fuhrmann SR, McGlinchey KA, Hammond SA, et al. Targeting CD73 in the tumor microenvironment with MEDI9447. Oncoimmunology 2016;5:e1208875.

5. Perrot I, Michaud HA, Giraudon-Paoli M, Augier S, Docquier A, Gros L, Courtois R, et al. Blocking Antibodies Targeting the CD39/CD73 Immunosuppressive Pathway Unleash Immune Responses in Combination Cancer Therapies. Cell Rep 2019;27:2411-2425 e2419.

6. Bowser JL, Broaddus RR. CD73s protection of epithelial integrity: Thinking beyond the barrier. Tissue Barriers 2016;4:e1224963.

7. Synnestvedt K, Furuta GT, Comerford KM, Louis N, Karhausen J, Eltzschig HK, Hansen KR, et al. Ecto-5'-nucleotidase (CD73) regulation by hypoxia-inducible factor-1 mediates permeability changes in intestinal epithelia. J Clin Invest 2002;110:993-1002.

8. Thompson LF, Eltzschig HK, Ibla JC, Van De Wiele CJ, Resta R, Morote-Garcia JC, Colgan SP. Crucial role for ecto-5'-nucleotidase (CD73) in vascular leakage during hypoxia. J Exp Med 2004;200:1395-1405.

9. Bowser JL, Blackburn MR, Shipley GL, Molina JG, Dunner K, Jr., Broaddus RR. Loss of CD73-mediated actin polymerization promotes endometrial tumor progression. J Clin Invest 2016;126:220-238.

10. Hart ML, Much C, Gorzolla IC, Schittenhelm J, Kloor D, Stahl GL, Eltzschig HK. Extracellular adenosine production by ecto-5'-nucleotidase protects during murine hepatic ischemic preconditioning. Gastroenterology 2008;135:1739-1750 e1733.

11. Snider NT, Griggs NW, Singla A, Moons DS, Weerasinghe SV, Lok AS, Ruan C, et al. CD73 (ecto-5'-nucleotidase) hepatocyte levels differ across mouse strains and contribute to mallory-denk body formation. Hepatology 2013;58:1790-1800.

12. Peng Z, Fernandez P, Wilder T, Yee H, Chiriboga L, Chan ES, Cronstein BN. Ecto-5'-nucleotidase (CD73) -mediated extracellular adenosine production plays a critical role in hepatic fibrosis. FASEB J 2008;22:2263-2272.

13. Fausther M, Sheung N, Saiman Y, Bansal MB, Dranoff JA. Activated hepatic stellate cells upregulate transcription of ecto-5'-nucleotidase/CD73 via specific SP1 and SMAD promoter elements. Am J Physiol Gastrointest Liver Physiol 2012;303:G904-914.

14. Global Burden of Disease Liver Cancer C, Akinyemiju T, Abera S, Ahmed M, Alam N, Alemayohu MA, Allen C, et al. The Burden of Primary Liver Cancer and Underlying Etiologies From 1990 to 2015 at the Global, Regional, and National Level: Results From the Global Burden of Disease Study 2015. JAMA Oncol 2017;3:1683-1691.

15. Sciarra A, Monteiro I, Menetrier-Caux C, Caux C, Gilbert B, Halkic N, La Rosa S, et al. CD73 expression in normal and pathological human hepatobiliopancreatic tissues. Cancer Immunol Immunother 2019.

16. Cohen S, Stemmer SM, Zozulya G, Ochaion A, Patoka R, Barer F, Bar-Yehuda S, et al. CF102 an A3 adenosine receptor agonist mediates anti-tumor and anti-inflammatory effects in the liver. J Cell Physiol 2011;226:2438-2447.

17. Stemmer SM, Benjaminov O, Medalia G, Ciuraru NB, Silverman MH, Bar-Yehuda S, Fishman S, et al. CF102 for the treatment of hepatocellular carcinoma: a phase I/II, open-label, dose-escalation study. Oncologist 2013;18:25-26.

18. Stemmer SM, Manojlovic NS, Marinca MV, Petrov P, Cherciu N, Ganea D, Ciuleanu T-E, et al. A phase II, randomized, double-blind, placebo-controlled trial evaluating efficacy and safety of namodenoson (CF102), an A3 adenosine receptor agonist (A3AR), as a second-line treatment in patients

with Child-Pugh B (CPB) advanced hepatocellular carcinoma (HCC). Journal of Clinical Oncology 2019;37:2503-2503.

19. Knapp K, Zebisch M, Pippel J, El-Tayeb A, Muller CE, Strater N. Crystal structure of the human ecto-5'-nucleotidase (CD73): insights into the regulation of purinergic signaling. Structure 2012;20:2161-2173.

20. Moremen KW, Tiemeyer M, Nairn AV. Vertebrate protein glycosylation: diversity, synthesis and function. Nat Rev Mol Cell Biol 2012;13:448-462.

21. Stowell SR, Ju T, Cummings RD. Protein glycosylation in cancer. Annu Rev Pathol 2015;10:473-510.

22. Snider NT, Altshuler PJ, Wan S, Welling TH, Cavalcoli J, Omary MB. Alternative splicing of human NT5E in cirrhosis and hepatocellular carcinoma produces a negative regulator of ecto-5'-nucleotidase (CD73). Mol Biol Cell 2014;25:4024-4033.

23. Strum JS, Nwosu CC, Hua S, Kronewitter SR, Seipert RR, Bachelor RJ, An HJ, et al. Automated assignments of N- and O-site specific glycosylation with extensive glycan heterogeneity of glycoprotein mixtures. Anal Chem 2013;85:5666-5675.

24. Tsou CC, Avtonomov D, Larsen B, Tucholska M, Choi H, Gingras AC, Nesvizhskii AI. DIA-Umpire: comprehensive computational framework for data-independent acquisition proteomics. Nat Methods 2015;12:258-264, 257 p following 264.

25. Thorsson V, Gibbs DL, Brown SD, Wolf D, Bortone DS, Ou Yang TH, Porta-Pardo E, et al. The Immune Landscape of Cancer. Immunity 2018;48:812-830 e814.

26. Chiu JH, Hu CP, Lui WY, Lo SC, Chang CM. The formation of bile canaliculi in human hepatoma cell lines. Hepatology 1990;11:834-842.

27. Fausther M, Lecka J, Soliman E, Kauffenstein G, Pelletier J, Sheung N, Dranoff JA, et al. Coexpression of ecto-5'-nucleotidase/CD73 with specific NTPDases differentially regulates adenosine formation in the rat liver. Am J Physiol Gastrointest Liver Physiol 2012;302:G447-459.

28. Llovet JM, Zucman-Rossi J, Pikarsky E, Sangro B, Schwartz M, Sherman M, Gores G. Hepatocellular carcinoma. Nat Rev Dis Primers 2016;2:16018.

29. Jemal A, Ward EM, Johnson CJ, Cronin KA, Ma J, Ryerson B, Mariotto A, et al. Annual Report to the Nation on the Status of Cancer, 1975-2014, Featuring Survival. J Natl Cancer Inst 2017;109.

30. Buisseret L, Pommey S, Allard B, Garaud S, Bergeron M, Cousineau I, Ameye L, et al. Clinical significance of CD73 in triple-negative breast cancer: multiplex analysis of a phase III clinical trial. Ann Oncol 2018;29:1056-1062.

31. Wettstein MS, Buser L, Hermanns T, Roudnicky F, Eberli D, Baumeister P, Sulser T, et al. CD73 Predicts Favorable Prognosis in Patients with Nonmuscle-Invasive Urothelial Bladder Cancer. Dis Markers 2015;2015:785461.

32. Koivisto MK, Tervahartiala M, Kenessey I, Jalkanen S, Bostrom PJ, Salmi M. Cell-type-specific CD73 expression is an independent prognostic factor in bladder cancer. Carcinogenesis 2019;40:84-92.

33. Shali S, Yu J, Zhang X, Wang X, Jin Y, Su M, Liao X, et al. Ecto-5'-nucleotidase (CD73) is a potential target of hepatocellular carcinoma. J Cell Physiol 2018.

34. Brown ZJ, Heinrich B, Greten TF. Mouse models of hepatocellular carcinoma: an overview and highlights for immunotherapy research. Nat Rev Gastroenterol Hepatol 2018;15:536-554.

35. Petrosyan A, Holzapfel MS, Muirhead DE, Cheng PW. Restoration of compact Golgi morphology in advanced prostate cancer enhances susceptibility to galectin-1-induced apoptosis by modifying mucin O-glycan synthesis. Mol Cancer Res 2014;12:1704-1716.

36. Resta R, Thompson LF. T cell signalling through CD73. Cell Signal 1997;9:131-139.

37. Airas L, Hellman J, Salmi M, Bono P, Puurunen T, Smith DJ, Jalkanen S. CD73 is involved in lymphocyte binding to the endothelium: characterization of lymphocyte-vascular adhesion protein 2 identifies it as CD73. J Exp Med 1995;182:1603-1608.

38. Mikhailov A, Sokolovskaya A, Yegutkin GG, Amdahl H, West A, Yagita H, Lahesmaa R, et al. CD73 participates in cellular multiresistance program and protects against TRAIL-induced apoptosis. J Immunol 2008;181:464-475.

39. Airas L, Niemela J, Salmi M, Puurunen T, Smith DJ, Jalkanen S. Differential regulation and function of CD73, a glycosyl-phosphatidylinositol-linked 70-kD adhesion molecule, on lymphocytes and endothelial cells. J Cell Biol 1997;136:421-431.

40. Dianzani U, Redoglia V, Bragardo M, Attisano C, Bianchi A, Di Franco D, Ramenghi U, et al. Co-stimulatory signal delivered by CD73 molecule to human CD45RAhiCD45ROlo (naive) CD8+ T lymphocytes. J Immunol 1993;151:3961-3970.

41. Puthenveedu MA, Bachert C, Puri S, Lanni F, Linstedt AD. GM130 and GRASP65-dependent lateral cisternal fusion allows uniform Golgi-enzyme distribution. Nat Cell Biol 2006;8:238-248.

42. Chang SH, Hong SH, Jiang HL, Minai-Tehrani A, Yu KN, Lee JH, Kim JE, et al. GOLGA2/GM130, cis-Golgi matrix protein, is a novel target of anticancer gene therapy. Mol Ther 2012;20:2052-2063.

43. Chia J, Goh G, Racine V, Ng S, Kumar P, Bard F. RNAi screening reveals a large signaling network controlling the Golgi apparatus in human cells. Mol Syst Biol 2012;8:629.

44. Mehta A, Herrera H, Block T. Glycosylation and liver cancer. Adv Cancer Res 2015;126:257-279.

45. Kim H, Kim K, Jin J, Park J, Yu SJ, Yoon JH, Kim Y. Measurement of glycosylated alpha-fetoprotein improves diagnostic power over the native form in hepatocellular carcinoma. PLoS One 2014;9:e110366.
46. Jiang K, Li W, Zhang Q, Yan G, Guo K, Zhang S, Liu Y. GP73 N-glycosylation at Asn144 reduces hepatocellular carcinoma cell motility and invasiveness. Oncotarget 2016;7:23530-23541.
47. Norton PA, Comunale MA, Krakover J, Rodemich L, Pirog N, D'Amelio A, Philip R, et al. N-linked glycosylation of the liver cancer biomarker GP73. J Cell Biochem 2008;104:136-149.
48. Cui J, Huang W, Wu B, Jin J, Jing L, Shi WP, Liu ZY, et al. N-glycosylation by N-acetylglucosaminyltransferase V enhances the interaction of CD147/basigin with integrin beta1 and promotes HCC metastasis. J Pathol 2018;245:41-52.
49. Park D, Xu G, Barboza M, Shah IM, Wong M, Raybould H, Mills DA, et al. Enterocyte glycosylation is responsive to changes in extracellular conditions: implications for membrane functions. Glycobiology 2017;27:847-860.

FIGURE LEGENDS

Figure 1. CD73 is highly expressed in malignant hepatocytes in human HCC. **A.** *NT5E* gene expression across tumors classified into the four major HCC immune sub-types: wound healing (C1), IFNγ-dominant (C2), inflammatory (C3), and lymphocyte depleted (C4). Data were obtained from the PanCancer Atlas. n.s.=no statistical significance in expression between groups (one-way ANOVA; Tukey's multiple comparisons test). **B.** Immunofluorescence analysis of CD73 (green) and DAPI-stained DNA (blue) in normal human liver (left), HCC adjacent (middle) and tumor tissue (right). Scale bars=50μm. **C.** Immunofluorescence analysis of CD73

(magenta), ZO1 (green) and DAPI-stained DNA (blue). Bottom panels represent boxed in areas of the merged images, revealing cytoplasmic (asterisk) and punctate perinuclear (arrowhead) clustering of CD73 in HCC tumor and adjacent tissue. In adjacent liver, CD73 was also localized in the lumen of the bile canaliculus (arrows). Scale bars=20μm. **D**. Immunofluorescence analysis of DAPI-stained DNA (blue), CD73 (green), and keratins K8 and K19 (red), which mark hepatocytes and cholangiocytes, respectively. Scale bars=50μm.

Figure 2. CD73 is endogenously expressed in human HCC cell lines and exhibits membrane and cytoplasmic expression. **A.** CD73 immunoblot and Coomassie stain (loading control) in HCC cell lines. **B.** Immunofluorescence staining of CD73 (green) and DNA (blue) in Huh7 (CD73-positive) and PLC/PRF5 (CD73-negative) cell lines. Scale bars=20μm**. C. C.** Immunofluorescence analysis of CD73 (magenta), ZO1 or Claudin-1 (green; as labeled in panels) and DAPI-stained DNA (blue) in Huh7 cells. Bottom panels represent boxed in areas of the merged images, revealing membrane (arrows) and punctate cytoplasmic (arrowheads) localization. Scale bars=40μm.

Figure 3. HCC tumor-specific CD73 biochemical alterations correlate with decreased 5′-nucleotidase activity. **A.** Representative immunoblot (top) of CD73 in adjacent liver (L) and tumor (T) OG lysates from surgical HCC specimens collected at the University of North Carolina (UNC). Coomassie-stained gel serves as a loading control. The numbers represent individual patients. **B.** Densitometric quantification of CD73 protein from immunoblot analysis of 23 pairs of adjacent liver and tumor tissues from HCC patients. **C.** Representative CD73 immunoblots of HCC adjacent liver (L) and tumor (T) tissue OG lysates from two patients demonstrating differences in tumor CD73 migration on SDS-PAGE. **D-F.** Distribution of HCC etiology (D), tumor stage (E), and fibrosis status (F) across tumor samples without CD73 shift (left bars; N=10) and with CD73 shift (right bars; N=12-13). Clinical and biochemical data on all samples are provided in Supplemental File 1. **G.** Measurement of 5′-nucleotidase activity in adjacent liver and tumor tissue OG lysates from HCC cases in which tumor CD73 did not exhibit a shift in migration (left panel; cases similar to #509 in C) and in HCC cases where there was a significant shift (right panel; cases similar to #275 in C). ****$p<0.0001$; paired t-test.

Figure 4. Site-specific glycan distribution on CD73 in normal human liver. A. Model of CD73 dimer structure (magenta) showing the four asparagine residues (yellow) that are targets of glycosylation. Structure of CD73 dimer was generated using Pymol (PDB: 4H1S). **B.** Effect of *in vitro* CD73 de-glycosylation using PNGaseF or Endo H. **C.** Relative abundance of glycans across the four CD73 N-linked glycosylation sites, demonstrating that N311 and N333 account for >70% of all glycans. *p<0.05; **p<0.01; ***p<0.001; one-way ANOVA Tukey's multiple comparisons test. **B.** Types of glycans present on the four CD73 glycosylation sites. GlcNAc ( ), mannose ( ), fucose ( ), galactose ( ), Neu5Ac ( ).

Figure 5. Site-specific increase in high mannose glycans promotes CD73 intracellular retention and decreased enzymatic activity. A. Percent of high mannose (top), hybrid (middle), and complex (bottom) glycans on CD73 extracted from normal liver (non-HCC; n=4), HCC adjacent liver (n=5) and HCC tumor tissue (n=5). *p<0.05; ***p<0.001; one-way ANOVA. **B-C.** Changes in glycan composition on the two major CD73 glycosylation sites, N311 and N333. **p<0.01; ***p<0.001; ****p<0.0001. **D.** Representative CD73 immunoblot (top) of PLC/PRF/5 cells transfected with empty vector, WT CD73 and non-glycosylatable mutants N311Q and N333Q demonstrating equal over-expression of CD73 protein. Measurement of 5′-nucleotidase activity (bottom) in lysates of control vector-transfected (-) or CD73-transfected PLC/PRF/5 cells. (n=3). Data are representative of at least 3 independent experiments. **p<0.01; ***p<0.001 (one-way ANOVA). **E.** Sub-cellular distribution of WT and glycosylation point mutant CD73 transfected in PLC/PRF/5 cells. Green=CD73; Blue=DNA. Scale bars=10µm. **F.** Co-localization between CD73-N333Q (green) and the Golgi marker protein GM130 (red). Scale bar=20µm.

Figure 6. Increased expression of the Golgi protein GM130 in HCC tumors correlates with global expression changes in *N*-linked glycoproteins-encoding genes. **A.** Immunoblot of Golgi-resident proteins GM130, Vti1, Syntaxin 6, and GS27 in HCC adjacent liver (L) and tumor (T) lysates. **B.** Quantification of the immunoblots in panel A. *p<0.05 compared to GS27; one-way ANOVA; Tukey's multiple comparisons test. **C.** Double immunofluorescence staining of GM130 (green) and DNA (blue) in adjacent liver and tumor tissue (representative images are from HCC case #752). Scale bars=50µm. Right panels show the respective magnified areas (represented by the yellow boxes). **D.** RNAseq analysis on four pairs of HCC adjacent liver-

tumors revealing the percentage (36-48%) of significantly differentially expressed genes that encode *N*-linked glycoproteins (complete dataset is in Supplemental File 2). **E.** RNA expression levels of select *N*-linked glycoprotein genes (ecto-nucleotidases *ENPP2* and *ENTPD8*, and *ADORA3*) in paired HCC adjacent liver (black bars) and tumor tissues (gray bars). Each bar represents a single readout from the RNAseq dataset (Supporting File 2). **F.** Summary of findings and working hypothesis model of HCC tumor-specific changes in *N*-glycosylation. HCC tumors exhibit altered Golgi structure, as exemplified by significant over-expression of the structural protein GM130. Changes in Golgi structure lead to altered localization and decreased function of *N*-linked glycoproteins, including ecto-nucleotidase CD73, and are associated with decreased expression of eNPP2, and eNTPD8, leading to overall decreased levels in the production of extracellular adenosine. Decreased adenosine production by the highly mannosylated tumor CD73 blunts adenosine-dependent HCC cell death via the A3 adenosine receptor, promoting HCC progression.

Supplemental Figure 1. Correlation analysis between biochemical changes of tumor-associated CD73 with disease presence/recurrence and patient survival. A-C. Correlation between CD73 tumor shift and patients' disease/vital status. Left bars; no shift in tumor CD73 (N=10). Right bars; shift in CD73 (N=13). **D-F**. Correlation between CD73 expression level and patients' disease/vital status. Left bars; tumor CD73 decreased (low) relative to adjacent liver (N=13). Right bars; tumor CD73 increased (high) relative to adjacent liver (N=6). Panels A and D represent distribution of patients who were never disease-free (black), patients who had successful tumor removal, but had disease recurrence (red), and patients who had successful tumor removal and did not have recurrence (blue). Panels B and E represent distribution of patients presenting with disease (red) or patients who had no evidence of disease (blue) at date of last contact. Panels C and F represent distribution of patients' vital status at date of last contact: deceased (dark blue); alive (light blue). P-values are noted below each comparison; Chi-square (panels A,D) and Fisher's exact test (panels B,C,D,E). Clinical and biochemical data on all samples is provided in Supporting File 1.

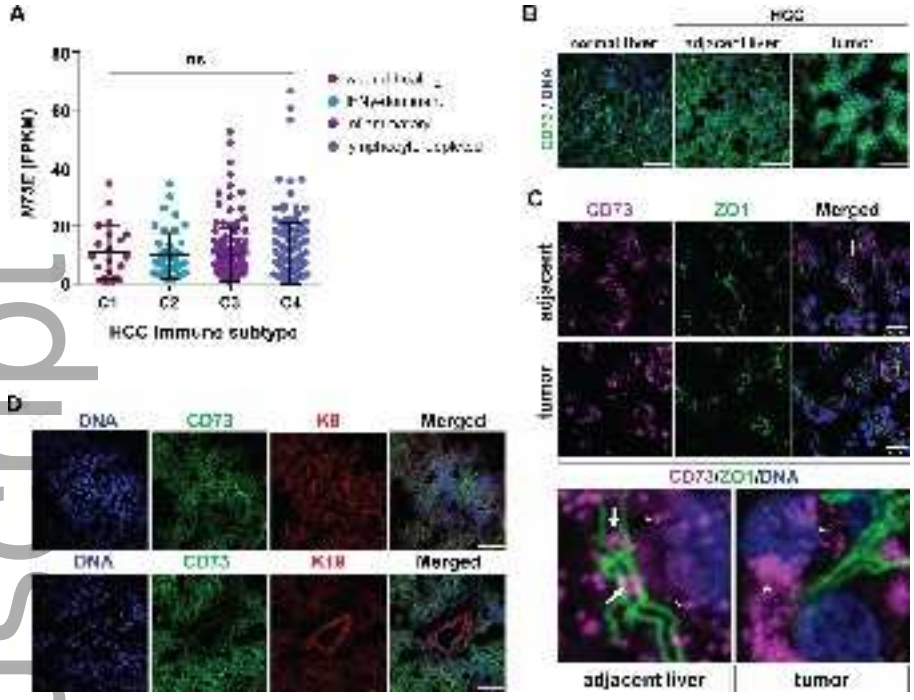

hep4_1410_f1.tif

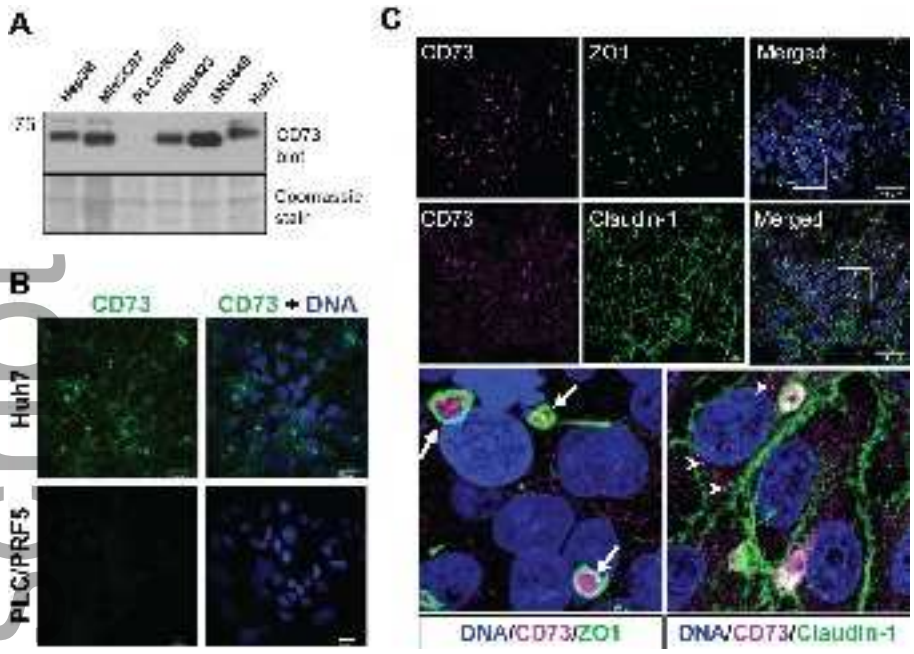

hep4_1410_f2.tif

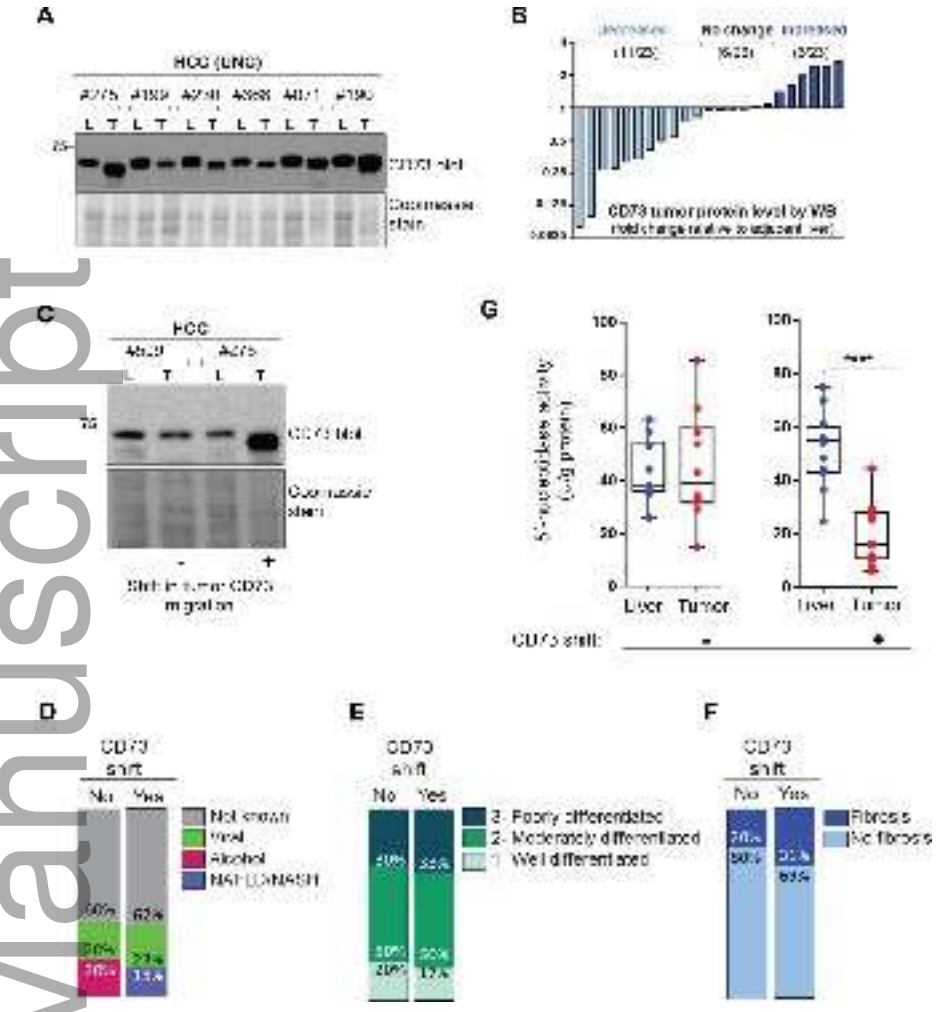

hep4_1410_f3.tif

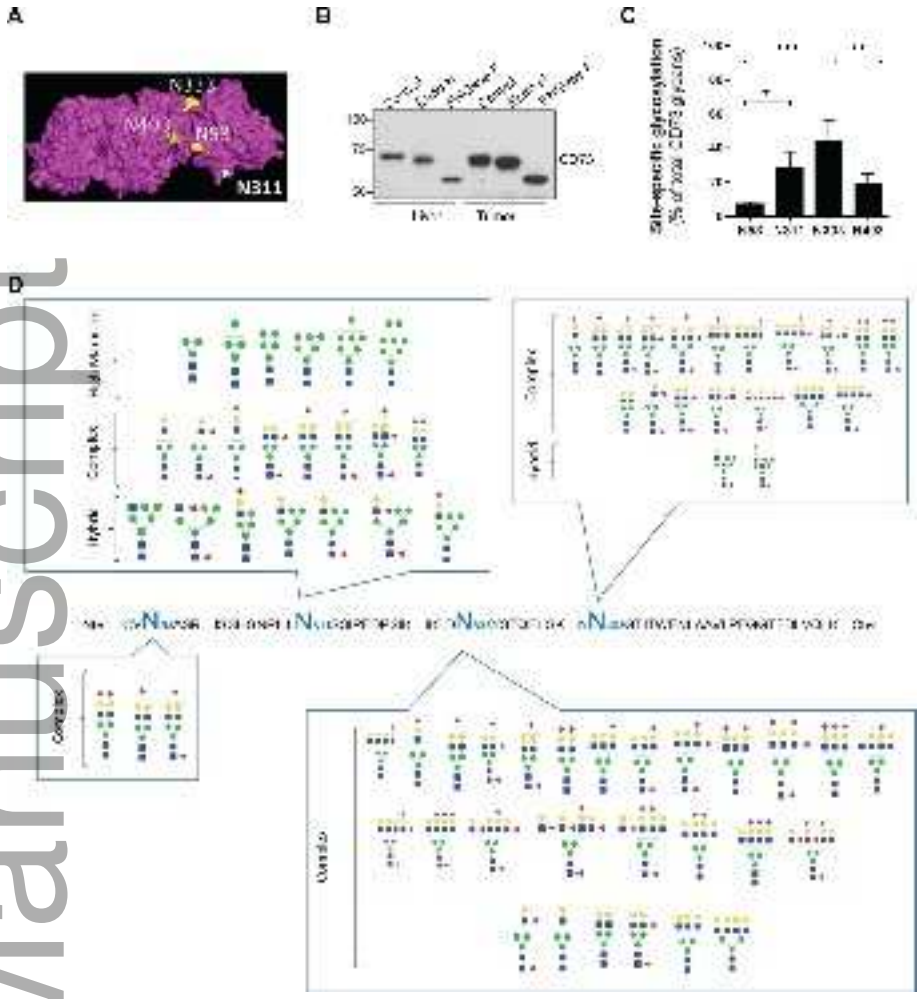

hep4_1410_f4.tif

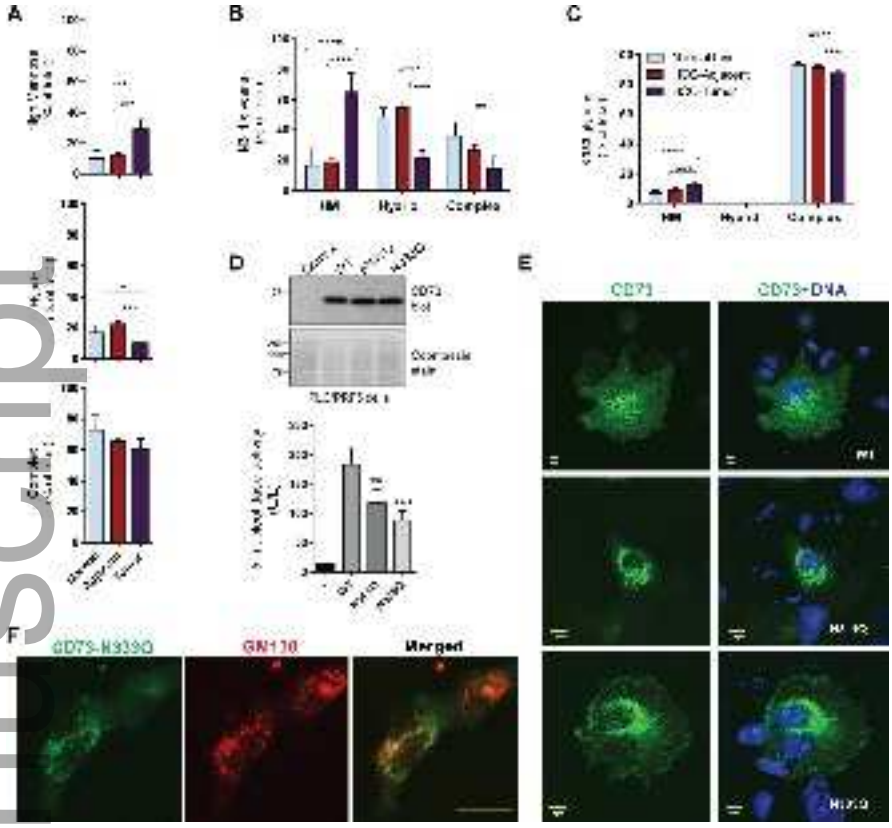

hep4_1410_f5.tif

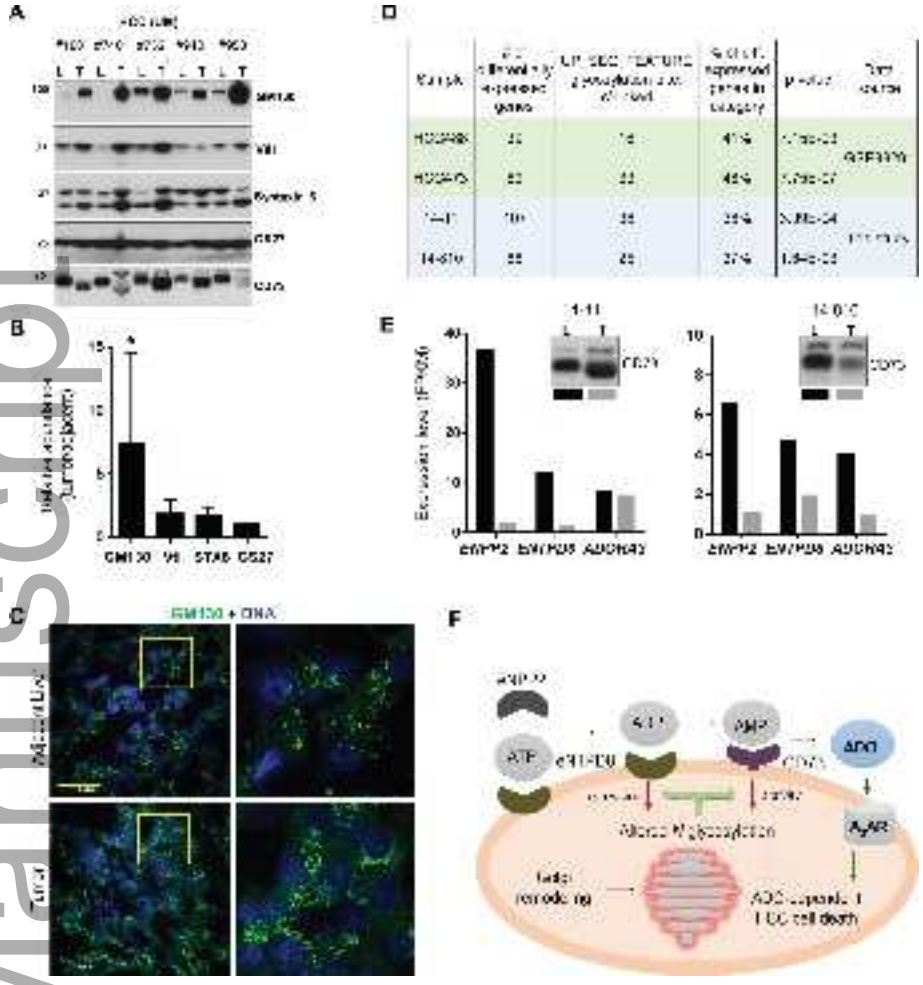

hep4_1410_f6.tif